

Electrical Transport Properties of Bi₂O₃-Doped CoFe₂O₄ and CoHo_{0.02}Fe_{1.98}O₄ Ferrites

Hasan Mehmood Khan*, Misbah-ul-Islam, Irshad Ali, Mazhar-ud-din Rana

Department of Physics, Bahauddin Zakariya University Multan, Multan, Pakistan.
Email: *hasan_bzu@yahoo.com

Received March 19th, 2011; revised April 26th, 2011; accepted May 6th, 2011.

ABSTRACT

Two series of CoHo_xFe_{2-x}O₄ (x = 0.0, 0.02) ferrites with Bismuth oxide doping from (0.1 - 0.3)% were prepared by Co-precipitation technique. X-ray diffraction analysis revealed fcc structure. The lattice constants were found to decrease as the doping of Bi₂O₃ increases in both series. An increase in Bismuth oxide concentration from (0.1 - 0.3%) in CoFe₂O₄ and CoHo_{0.02}Fe_{1.98}O₄ ferrites leads to an increase in room temperature resistivity. Temperature dependent resistivity decreases as the temperature increases following the Arrhenius equation. The activation energy increases with the increase of Bi₂O₃-concentration for both CoFe₂O₄ and CoHo_{0.02}Fe_{1.98}O₄ series. The frequency dependant dielectric constant follows the Maxwell-Wagner type interfacial polarization. The dielectric loss indicates the normal behavior of these ferrites. SEM analysis shows an increase in grain size with increasing Bismuth concentration.

Keywords: Cobalt Ferrites, Co-Precipitation, Bi Doping, Electrical Properties

1. Introduction

The miniaturization of electrical and electronic gadgets demands new materials with nano-size particles for high frequency applications and high density recording. Bi₂O₃ is a potential dopant for improving the magnetic and electrical properties of ferrites. The properties of ferrite materials are known to be strongly influenced by their composition and microstructure which are sensitive to the processing methods used to synthesize them. Over the last decade, the magnetostrictive materials for smart sensors have attracted a great interest due to their wide range of applications in the automotive industry. The cobalt ferrites are well known for its highest magnetostrictive coefficient amongst the oxide-based magnetostrictive materials. Cobalt ferrite nanoparticles have recently become the subject of research interest from the point of view of the synthesis, the magnetic characterization, and the applications [1-4]. Among the various ferrite materials for magnetic recording applications, cobalt ferrite (CoFe₂O₄) has been widely studied [5]. Cobalt ferrite (CoFe₂O₄) possesses excellent chemical stability, good mechanical hardness and a large positive first-order crystalline anisotropy constant, which made this ferrite a promising candidate for magneto-optical recording media [6]. High electrical resistivity and low eddy current

losses make these ferrites an excellent core material for power transformers in electrical and electronic industry, recording heads, antenna rods, loading coils, microwave devices and telecommunication applications [7,8]. The magnetic properties of ferrites can be modified by introducing suitable divalent and trivalent oxides as dopants [9]. It is reported [10] the dc electrical conductivity of the Bi₂O₃-doped ferrites was increased. Bi₂O₃ is an alternative sintering aid for lowering sintering temperature of magnesium ferrites. The addition of Bi₂O₃ has significant effect on the resistivity and dielectric properties of ferrites. Moreover the advantageous effect of Bi₂O₃ is attributed to the formation of liquid phase layer due to the low melting point of Bi₂O₃ [11] which enhances the resistivity of the ferrites. Due to the presence of Bi₂O₃ the properties of grain boundaries of ferrite were changed and three dimensional network grain boundary structure formed at grain boundaries [12-15]. Since Bi₂O₃ doping enhances the magnetic and electrical properties of the ferrites, the purpose of this study is to investigate the influence of the Bi₂O₃ doping from 0.1-0.3% by weight on the microstructure, electrical and magnetic properties of CoFe₂O₄ and CoHo_{0.02}Fe_{1.98}O₄ ferrites. The CoHo_{0.02}-Fe_{1.98}O₄ was chosen for comparison between CoFe₂O₄ and the Rare earth substituted CoHo_{0.02}Fe_{1.98}O₄ ferrites after doping Bi₂O₃.

2. Experimental

Bi₂O₃ doped CoFe₂O₄ (Bi₂O₃:0.1 - 0.3%) and CoHo_{0.02}-Fe_{1.98}O₄ (Bi₂O₃:0.1 - 0.3%) ferrites were prepared by using co-precipitation method. The starting materials 99.9% pure, Co(C₂H₃O₂)₂, FeCl₃ and Ho₂O₃ were used. The stoichiometric amounts of selected salts were dissolved in de-ionized water in a 100ml beaker except Ho₂O₃ which is insoluble in de-ionized water. Ho₂O₃ was dissolved in HCl heated at 50 - 60°C and then added in the solution. The solution so obtained was stirred using magnetic stirrer for 10 hrs. During stirring calculated amount of Na₂CO₃/NaOH were used in the solution as reagent or as precipitating agents to precipitate the metals and hydroxides. The precipitates were thoroughly washed with distilled water until free from chloride ions, which were checked by AgNO₃ test. The final product was then filtered with the help of suction flask having an outlet with pump operated on water. The filtered precipitates were dried in oven for 24h at 100°C. The dried precipitates were then ground in mortar and pestle and Bi₂O₃ was then doped from (0.1 - 0.3) wt% in both set of samples during grinding. The Pellets of ground powders were formed using Paul-Otto Weber hydraulic press under the pressure of (~35 KN·mm²). The pellets were then sintered in an electric furnace at 1150 - 1200°C for 10h followed by furnace cooling. For electrical measurements both surfaces of the pellets were polished on the micron paper. The phase formation of the samples was investigated by Shimadzu X-ray diffractometer using CuK_α radiations ($\lambda = 1.5406\text{\AA}$). SEM analysis of the one series of samples was investigated by JEOL-Japan Model JSM 5910 and it was used to observe the microstructure of the sintered specimens. Electrical resistivity was measured by two probe method using source meter model 2400 (Keithley). The dielectric properties were measured using Digi Bridge (GenRad 1689).

3. Results and Discussions

3.1. X-Ray Diffraction

X-ray diffraction patterns of Bi₂O₃ doped CoFe₂O₄ (Bi₂O₃:0.1 - 0.3%) and CoHo_{0.02}Fe_{1.98}O₄ (Bi₂O₃:0.1 - 0.3%) ferrites are shown in **Figures 1(a,b)** respectively. The X-ray diffraction analysis shows the formation of single phase fcc spinel crystal structure for all the samples. The d-values were compared using JCPDS (1998) cards (card No. 01 - 1121) [16]. Apparently no traces of secondary phase were observed [17-19]. The 220, 311, 400, 333, 440 reflections were observed in X-ray diffraction patterns.

3.2. Lattice Constant

The lattice constants of CoFe₂O₄ (Bi₂O₃: 0.1 - 0.3%) and CoHo_{0.02}Fe_{1.98}O₄ (Bi₂O₃: 0.1 - 0.3%) samples are shown in

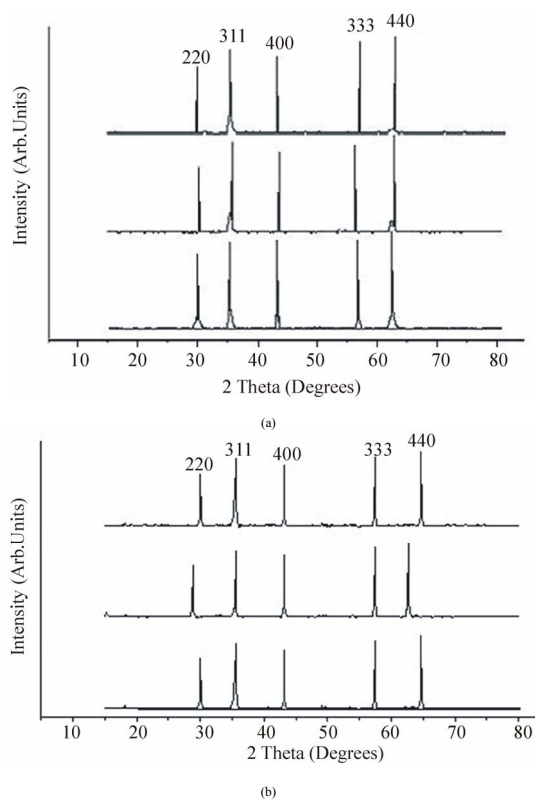


Figure 1. (a) XRD pattern for CoFe₂O₄ (Bi₂O₃: 0.1 - 0.3%). (b) XRD pattern for CoHo_{0.02}Fe_{1.98}O₄ (Bi₂O₃: 0.1 - 0.3%)

Figures 2(a,b). It is observed that the lattice constants decrease as the doping of Bi₂O₃ increases. The decrease in 'a' is due to the difference in ionic radii of Bi³⁺ (0.74Å) as compared to Fe³⁺ (0.78Å) [7]. The decrease in lattice constant in both series can be explained on the basis of the fact that the Bi₂O₃ enter into the lattice completely during sintering due to very small amount of Bi₂O₃ doping.

3.3. Room Temperature Resistivity

Figures 3(a,b) shows the room temperature resistivity versus Bi₂O₃ concentration for both CoFe₂O₄ and CoHo_{0.02}Fe_{1.98}O₄ ferrite series. It can be observed that as Bi₂O₃-concentration increases, the resistivity increases from 18×10^4 to a maximum value of $42 \times 10^4 \Omega\text{-cm}$ for CoFe₂O₄, (Bi₂O₃: 0.1 - 0.3%) samples and from 7×10^3 to $32 \times 10^4 \Omega\text{-cm}$ for CoHo_{0.02}Fe_{1.98}O₄ (Bi₂O₃: 0.1 - 0.3%) ferrites. The increase in Bi₂O₃ concentration leads to an increase in resistivity that might be due to the fact that Bi⁵⁺ act as scattering centres for the carriers hopping between two octahedral sites [7,10], which hinders the hopping mechanism between the Fe²⁺ and Fe³⁺ ions.

3.4. Temperature Dependant Resistivity

Temperature dependent electrical resistivity of CoFe₂O₄

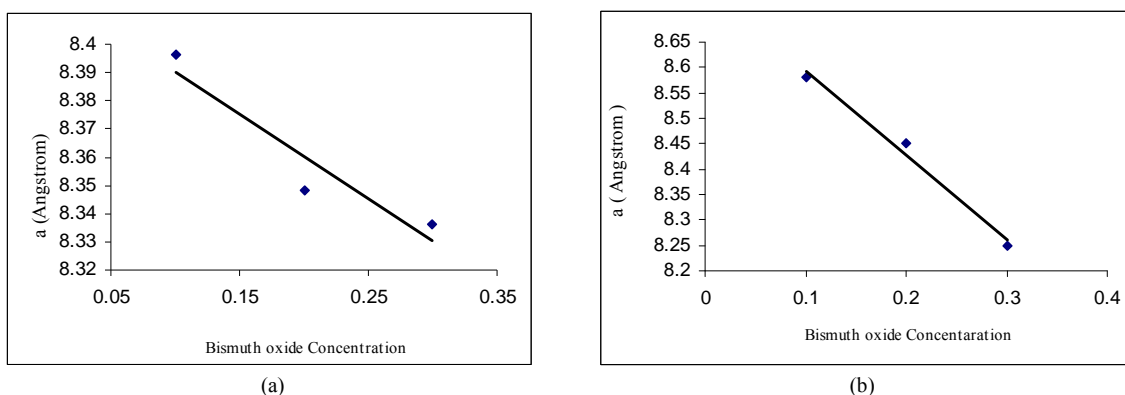


Figure 2. (a) Lattice constant for CoFe₂O₄, (Bi₂O₃: 0.1 - 0.3%); (b) Lattice constant for CoHo_{0.02}Fe_{1.98}O₄, (Bi₂O₃: 0.1 - 0.3%).

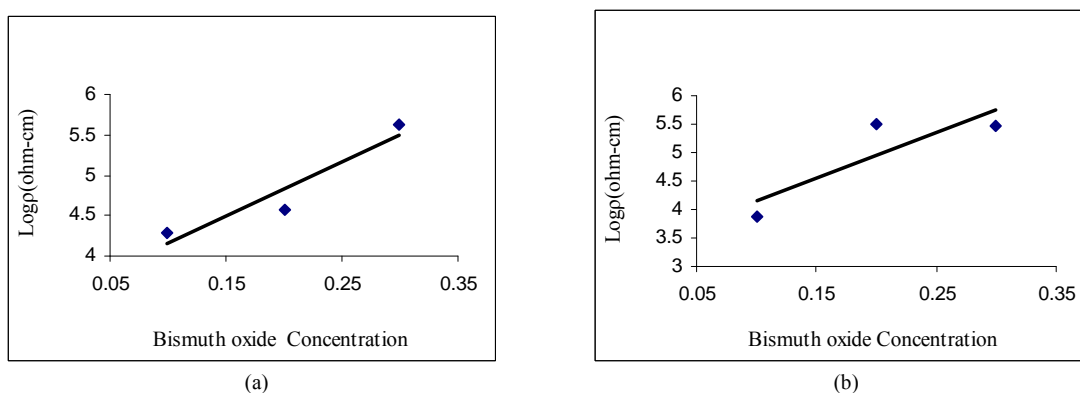
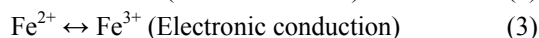
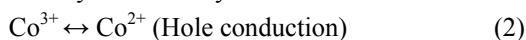


Figure 3. (a) Room temperature resistivity (ρ) for CoFe₂O₄, (Bi₂O₃: 0.1% - 0.3%); (b) Room temperature resistivity (ρ) for CoHo_{0.02}Fe_{1.98}O₄, (Bi₂O₃: 0.1% - 0.3%).

(Bi₂O₃:0.1 - 0.3%) and CoHo_{0.02}Fe_{1.98}O₄ (Bi₂O₃:0.1-0.3%) ferrite series was measured in temperature range (40 - 200°C). The Arrhenius plots of these samples are shown in **Figures 4(a)** and **(b)** respectively. Each sample follows Arrhenius equation,

$$\rho = \rho_0 \exp \frac{\Delta E}{K_B T} \quad (1)$$

where ΔE is the activation energy, T is the absolute temperature, k_B is the Boltzmann's constant. The plots show that the resistivity decreases as the temperature increases indicating the semi conducting nature of the samples [10]. This decrease in resistivity may be due to the excess of electrons released from both sites which reduces the Co²⁺ to their lowest valency and also produce Fe²⁺ ions [20]. The behavior of both type of electric charge carriers can be explained on the basis of Rezlescu model [21]. According to this model, the exchanging of electrons between Fe²⁺ and Fe³⁺ ions and that of holes between Co³⁺ to Co²⁺ ions may be the likely conduction mechanism.



3.5. Activation Energy

The activation energy obtained from Arrhenius plots are

shown in **Figures 5(a,b)** respectively. The activation energy increases with the increase of Bi₂O₃-concentration for both CoFe₂O₄ and CoHo_{0.02}Fe_{1.98}O₄ samples. It can be observed that the samples having high resistivity value also have high activation energy and vice versa [22]. The result indicates the presence of conduction dependant to the structure [23]. As the activation energy is high and so the resistivity is high due to which conductivity will be lower as Bi₂O₃ is substituted which can be thought of due to phonon-assisted small polaron hopping [21-22].

3.6. Drift Mobility

Figures 6(a) and **(b)** respectively shows the variation of drift mobility with temperature for both series. The drift mobility was calculated by using the resistivity data and is calculated with the help of the given formula [23-25].

$$\mu_d = 1/nep \quad (4)$$

where ρ is electrical resistivity, e is charge on an electron and ' n ' is the concentration of charge carriers and it is calculated by following relation;

$$n = N_A C_{Fe} \rho_b / M \quad (5)$$

where N_A is Avogadro's number, C_{Fe} is the number of iron atoms in sample, ρ_b is the bulk density and M is the

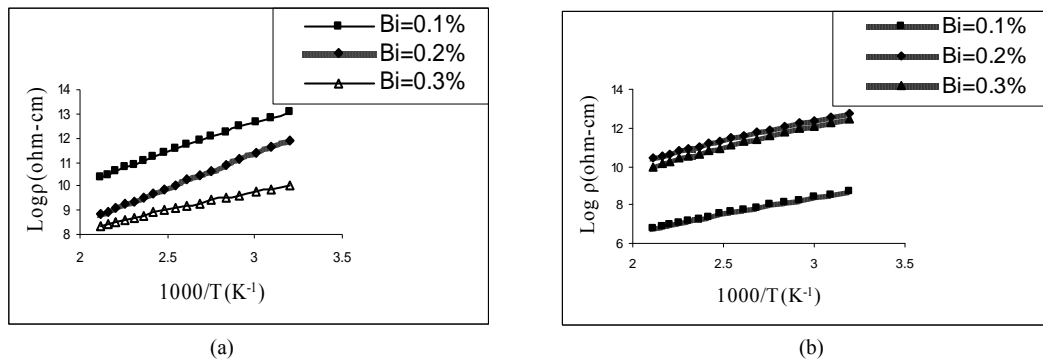


Figure 4. (a) Temperature dependant resistivity for CoFe_2O_4 , (Bi_2O_3 : 0.1% - 0.3%); (b) Temperature dependant resistivity for $\text{CoHo}_{0.02}\text{Fe}_{1.98}\text{O}_4$, (Bi_2O_3 : 0.1% - 0.3%)

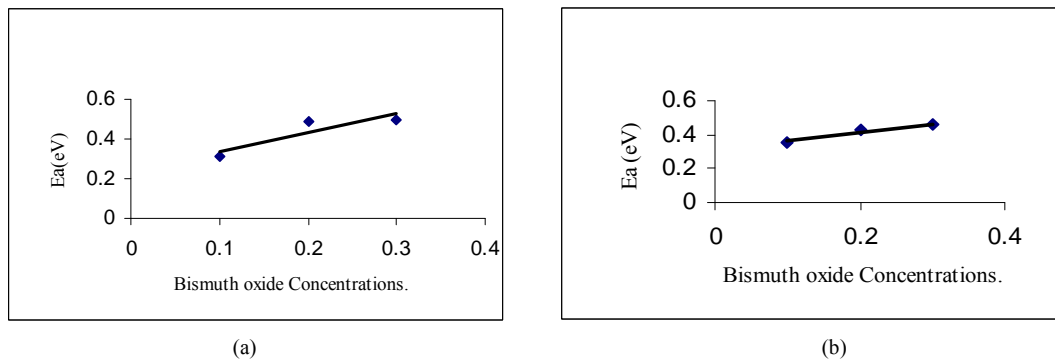


Figure 5. (a) Activation Energy for CoFe_2O_4 , (Bi_2O_3 : 0.1% - 0.3%); (b) Activation Energy $\text{CoHo}_{0.02}\text{Fe}_{1.98}\text{O}_4$, (Bi_2O_3 : 0.1% - 0.3%).

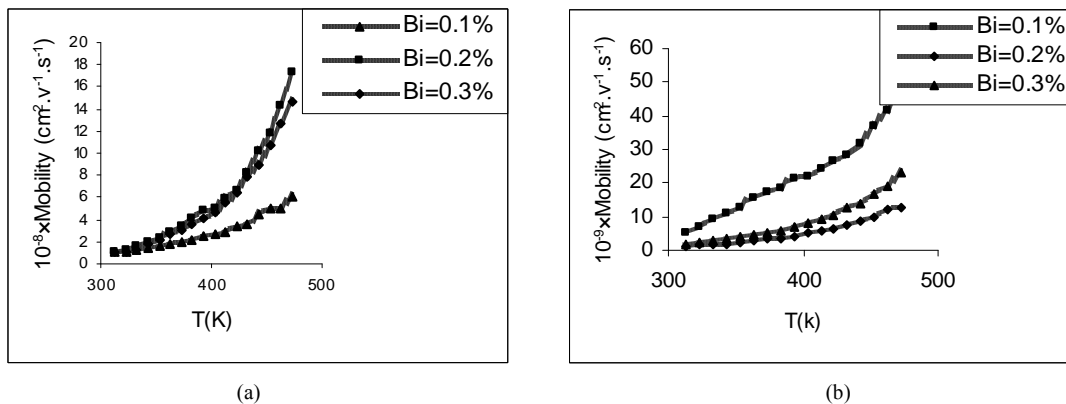


Figure 6. (a) Drift Mobility for CoFe_2O_4 , (Bi_2O_3 : 0.1% - 0.3%); (b) Drift Mobility for $\text{CoHo}_{0.02}\text{Fe}_{1.98}\text{O}_4$, (Bi_2O_3 : 0.1% - 0.3%).

molar mass of the samples. It is however observed that drift mobility increases with the increase in temperature. This may be due to the fact that charge carriers start hopping from one site to another as the temperature increases [26]. The temperature dependence of resistivity and mobility shows that the samples are of degenerate type semiconductors.

3.7. Dielectric Properties

3.7.1. Dielectric Constant and Loss Tangent

The dielectric constant Vs frequency of both the series at

room temperature 30°C are shown in **Figures 7(a,b)** respectively. The dielectric constant decreases with increasing frequency. At high frequencies the dielectric constant seems to be independent of frequency. This behavior of the samples is in accordance with the Maxwell Wagner model [27-29]. In this model the dielectric structure of ferrite material is assumed to be made up of two layers. First layer being conducting, contains large number of grains and other being grain boundaries which are poor conductor. This bi-layer formation is resulted by high temperature sintering [23]. **Figures 8(a,b)** shows

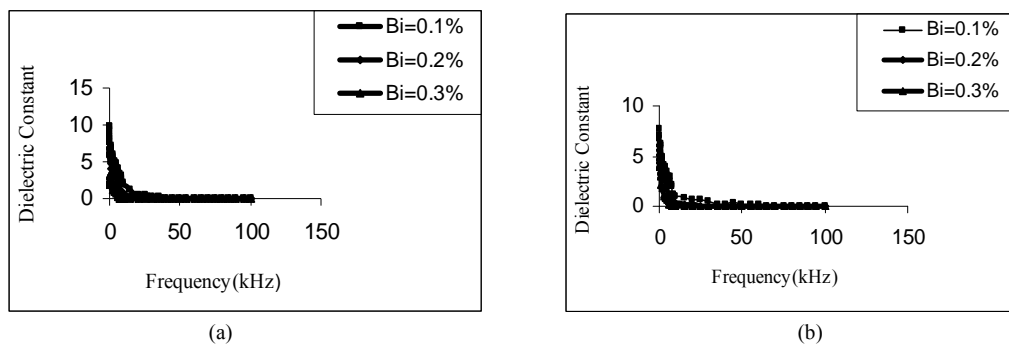


Figure 7. (a) Dielectric Constant vs Frequency for CoFe₂O₄, (Bi₂O₃: 0.1 - 0.3%); (b) Dielectric Constant vs Frequency for CoHo_{0.02}Fe_{1.98}O₄, (Bi₂O₃: 0.1 - 0.3%).

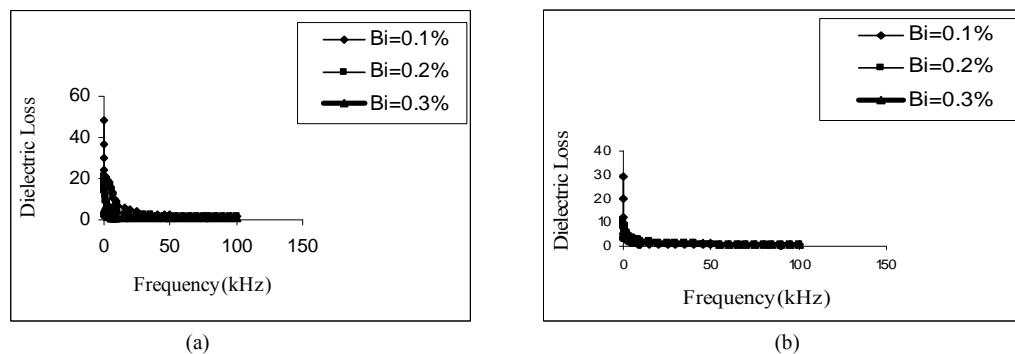


Figure 8. (a) Dielectric vs Frequency loss for CoFe₂O₄, (Bi₂O₃: 0.1% - 0.3%); (b) Dielectric Loss vs Frequency for CoHo_{0.02}Fe_{1.98}O₄, (Bi₂O₃: 0.1% - 0.3%).

$\tan\delta$ Vs frequency for both series. The dielectric loss decreases substantially with increasing frequency and reaches a constant value later on [30-32]. When the frequency of applied field is low than the hopping frequency of electrons between ferrous and ferric ions at adjacent octahedral sites, the electron follow the applied field and hence loss is maximum. At higher frequencies the hopping frequency of the electron exchange between ferrous and ferric ions can not follow applied field beyond certain critical frequency and the loss is minimum.

3.8. Scanning Electron Microscopy

Few representative SEM micrographs of CoFe₂O₄ (Bi₂O₃: 0.1% - 0.3%) are shown in **Figures 9 (a,b,c)** respectively. The grain boundaries and grains can be clearly distinguished at 50,000 magnification. The SEM micrographs of the CoFe₂O₄ (Bi₂O₃: 0.1% - 0.3%) sintered at 1150°C for 10 h are shown for various contents of Bi₂O₃. It is however observed that the grain size increases from 141 - 201 nm with the increase in Bi₂O₃ concentration in CoFe₂O₄ (Bi₂O₃: 0.1% - 0.3%) ferrites. Uneven grain boundaries were also observed. These non-uniform grain boundaries seems to be a diffusion induced grain boundary migration [33,34].

4. Conclusions

1) X-ray diffraction analysis reveals that CoFe₂O₄

(Bi₂O₃:0.1% - 0.3%) and CoHo_{0.02}Fe_{1.98}O₄ (Bi₂O₃: 0.1% - 0.3%) ferrite series clearly indicate formation of spinel fcc single phase crystal structure. The lattice constant 'a' decreases as Bi₂O₃ concentration increases for both series due to the difference in the ionic radii.

2) Room temperature dc resistivity of both series of ferrites increases due to the formation of Bi⁵⁺ ions.

3) The temperature dependant resistivity and activation energy Vs Bi content follows same trend indicating that the samples with high resistivity have high activation energies and vice versa .

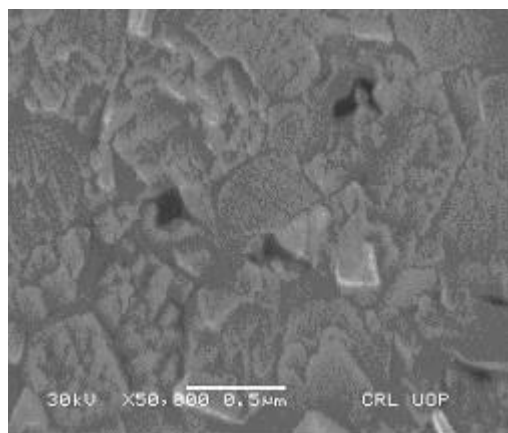
4) The behavior of dielectric constant and loss tangent for both series of ferrite follows the Maxwell Wagner model.

5) The SEM micrographs of the CoFe₂O₄ (Bi₂O₃: 0.1% - 0.3%) ferrites shows that the grain size increases from 141 - 201 nm with the increase in Bi₂O₃ concentration.

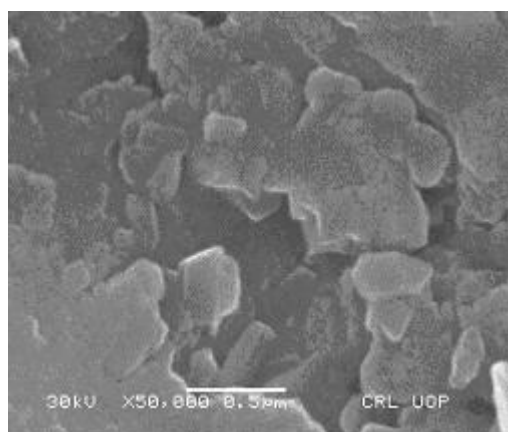
6) The activation energy shows that the hopping conduction mechanism is established in these samples.

5. Acknowledgements

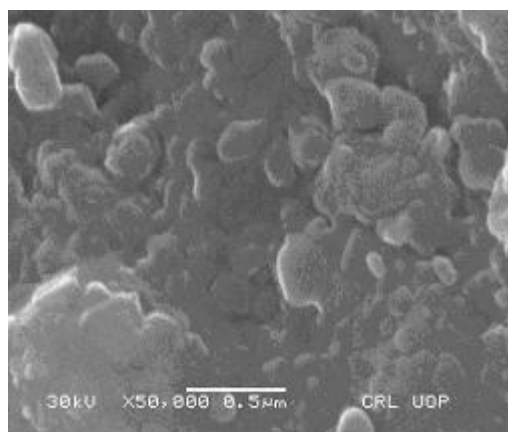
Authors are thankful to Higher Education Commission of Pakistan for providing financial assistance under 5000 indigenous fellowship programme. We are grateful to Dr. Amir Bashir Ziya for his help in taking XRD patterns of the samples.



(a)



(b)



(c)

Figure 9. (a) SEM for CoFe_2O_4 (Bi_2O_3 : 0.1%); (b) SEM for CoFe_2O_4 (Bi_2O_3 : 0.2%); (c) SEM for CoFe_2O_4 , (Bi_2O_3 : 0.3%).

REFERENCES

- [1] C. Hou, H. Yu, Q. Zhang, Y. Li, and H. Wang, "Preparation and Magnetic Property Analysis of Monodisperse Co-Zn Ferrite Nanospheres," *Journal Alloys Compounds*, Vol. 491, No. 1-2, 2010, pp. 431-435.
- [2] R. C. Kambale, P. A. Shaikh, N. S. Harale, V. A. Bilur, Y. D. Kolekar, C. H. Bhosale and K. Y. Rajpure, "Conductivity Study of Polyaniline-Cobalt Ferrite ($\text{PANI-CoFe}_2\text{O}_4$) Nanocomposite," *Journal Alloys Compounds*, Vol. 490, No. 2, 2010, pp. 568-571.
[doi:10.1016/j.jallcom.2009.10.082](https://doi.org/10.1016/j.jallcom.2009.10.082)
- [3] L. Ai and J. Jiang, "Influence of Annealing Temperature on the Formation, Microstructure and Magnetic Properties of Spinel Nanocrystalline Cobalt Ferrites," *Current Applied Physics*, Vol. 10, No. 1, 2010, pp. 284-288.
[doi:10.1016/j.cap.2009.06.007](https://doi.org/10.1016/j.cap.2009.06.007)
- [4] B. E. Kashevsky, V. E. Agabekov, S. B. Kashevsky, K. A. Kekalo, E. Y. Manina, I. V. Prokhorov and V. S. Ulashchik, "Study of Cobalt Ferrite Nanosuspensions for Low-Frequency Ferromagnetic Hyperthermia," *Particuology*, Vol. 6, No. 5, 2008, pp. 322-333.
[doi:10.1016/j.partic.2008.07.001](https://doi.org/10.1016/j.partic.2008.07.001)
- [5] A. E. Berkowitz and W. Schuele, "Properties of Some Ferrite Micropowders," *Journal Applied Physics*, Vol. 30, No. 4, 1959, pp. 134S-135S. [doi:10.1063/1.2185853](https://doi.org/10.1063/1.2185853)
- [6] M. Pal, P. Brahma and D. Chakravorty, "Magnetic and Electrical Properties of Nickel-Zinc Ferrites Doped with Bismuth Oxide," *Magnetism Magnetic Materials*, Vol. 152, No. 3, 1996, pp. 370-374.
- [7] M. A. El Haiti, *Magnetism and Magnetic Materials*, Vol. 136, 1994, pp. 138-141.
- [8] P. Brahma, A. K. Giri, D. Chakravorty, M. Tiwari and D. Bahadur, "Magnetic Properties of Sb_2O_3 -Doped Ba-M Hexagonal Ferrites," *Magnetism Magnetic Materials*, Vol. 102, 1991, pp. 109-115.
- [9] M. Pal, P. Brahma, B. R. Chakravorty and D. Chakravorty, "DC Conductivity in Barium Hexaferrites Doped with Bismuth Oxide," *Japanese Journal Applied Physics*, Vol. 36, No. 4A, 1997, pp. 2163-2166.
[doi:10.1143/JJAP.36.2163](https://doi.org/10.1143/JJAP.36.2163)
- [10] L. B. Kong, Z. W. Li, G. Q. Lin and Y. B. Gan, "Electrical and Magnetic Properties of Magnesium Ferrite Ceramics Doped with Bi_2O_3 ," *Acta Material*, Vol. 55, No. 19, 2007, pp. 6561-6572.
[doi:10.1016/j.actamat.2007.08.011](https://doi.org/10.1016/j.actamat.2007.08.011)
- [11] J. Wong, "Sintering and Varistor Characteristics of ZnO- Bi_2O_3 Ceramics," *Applied Physics*, Vol. 51, No. 8, 1980, pp. 4453-4458.
[doi:10.1063/1.328266](https://doi.org/10.1063/1.328266)
- [12] W. D. Kingery, H. K. Bowen and D. R. Uhlmann, "Clinical Decisions to Limit Treatment," Introduction to ceramics, 2nd Edition, John Wiley, New York, Vol. 2, 1976, pp. 913-945.
- [13] A. Verma and D. C. Dube, "Processing of Nickel-Zinc Ferrites via the Citrate Precursor Route for High-Frequency Applications," *Journal American Ceramic Society*, Vol. 88, No. 3, 2005, pp. 519-526.
[doi:10.1111/j.1551-2916.2005.00098.x](https://doi.org/10.1111/j.1551-2916.2005.00098.x)
- [14] D. R. Clarke, "Varistor Ceramics," *Journal American Ceramic Society*, Vol. 82, No. 3, 1999, pp. 485-492.

[doi:10.1111/j.1151-2916.1999.tb01793.x](https://doi.org/10.1111/j.1151-2916.1999.tb01793.x)

- [15] JCPDS-International, "Centre for Diffraction," *Data PCPDFWIN*, Vol. 2, No. 1, 1998, pp. 11-21.
- [16] S. T. Mahmud, A. K. M. Akhter Hussain, A. K. M. Abdul Hakim, M. Seki, T. Kawai and H. Tabata, "Influence of Microstructure on the Complex Permeability of Spinel Type Ni Zn Ferrite," *Magnetism Magentic Materials*, Vol. 305, No. 1, 2006, pp. 269-274.
- [17] F. G. Chang, G. L. Song, K. Fang, P. Qin and Q. J. Zeng, "Effect of Gadolinium Substitution on Dielectric Properties of Bismuth Ferrite," *Journal of Rare Earths, Special Issue*, Vol. 24, 2006, pp. 273-276.
[doi:10.1016/S1002-0721\(07\)60379-2](https://doi.org/10.1016/S1002-0721(07)60379-2)
- [18] K. J. D. Mackenzie, T. Dougherty, and J. Barrel, "The Electronic Properties of Complex Oxides of Bismuth with the Mullite Structure," *Journal of the Euorpean Ceramic Society*, Vol. 28, No. 2, 2008, pp. 499-504.
[doi:10.1016/j.jeurceramsoc.2007.03.012](https://doi.org/10.1016/j.jeurceramsoc.2007.03.012)
- [19] U. Ghazanfar, S. A. Siddiqi and G. Abbas, "Study of Room Temperature Dc Resistivity in Comparison with Activation Energy and Drift Mobility of NiZn Ferrites," *Materials Science and Engineering B*, Vol. 118, No. 2, 2005, pp. 132-134.
- [20] N. Rezlescu and E. Rezlescu, "Study of Room Temperature Dc Resistivity in Comparison with Activation Energy and Drift Mobility of NiZn Ferrites," *Physics Status Solid A*, Vol. 23, No. 2, 1974, pp. 575-579.
[doi:10.1002/pssa.2210230229](https://doi.org/10.1002/pssa.2210230229)
- [21] N. F. Mott and J. Non-Cryst, "Dissertation," *Solids*, Vol. 1, 1968, pp. 1-17.
- [22] D. S. Birajdar, D. R. Mane, S. S. More, V. B. Kawade, and K. M. Jadhav, "Structural and Magnetic Properties of Zn_xCu_{4-x}Mn_{0.4}Fe₂O₄ Ferities," *Journal Material*, Vol. 59, No. 24-25, 2005, pp. 2981-2985.
- [23] L. Nalbandian, A. Delimitis, V. T. ZaspaliS, E. A. Deliyani, D. N. Bakoyannakis, E. N. Pelek and A. J. Micropor, "Hydrothermally Prepared Nanocrystalline Mn-Zn Ferrites: Synthesis and Characterization," *Mesoporous Material*, Vol. 114, No. 1-2, 2008, pp. 465-473.
- [24] M. K. Shobanaa, S. Sankara, V. Rajendranb, M. K. Shobanaa, S. Sankara and V. Rajendranb, "Shape and Director Field Deformation of Tactoids," *Masterial Chemistry Physics*, Vol. 113, No. 12, 2009, pp. 10-13.
[doi:10.1016/j.matchemphys.2008.07.083](https://doi.org/10.1016/j.matchemphys.2008.07.083)
- [25] M. N. Ashiq, N. Bibi and M. A. Malana, "Effect of Sn-Ni Substitution on the Structural, Electrical and Magnetic Properties of Mixed Spinel Ferrites," *Journal of Alloys and Compounds*, Vol. 490, No. 1-2,4 February 2010, pp. 594-597.
- [26] K. C. Maxwell, "Electricity and Magnetism," Oxford University Press, London, Vol. 1, 1873, pp. 328-332.
- [27] K. W. Wagner, "A Biliography of Zimbabwean Archaeology to 2005," *Journal American Creamic Society*, Vol. 40, 1913, pp. 817-823.
- [28] L. T. Robinkin and Z. I. Novikova, "Ferrites," *IZV Academics Nauk USSR, Minisik*, 1960, pp. 146-152.
- [29] V. R. K. Murthy and J. Shobanadri, "Dielectric Properties of Some Nickel-Zinc Ferrites at Radio Frequency," *Physics Status Solid A*, Vol. 36, No. 2, 1976, pp. 133-140.
[doi:10.1002/pssa.2210360247](https://doi.org/10.1002/pssa.2210360247)
- [30] N. Rezlescu and E. Rezlescu, " Physics Status Solid A, Vol. 23, 1974, pp. 575-581.
[doi:10.1002/pssa.2210230229](https://doi.org/10.1002/pssa.2210230229)
- [31] K. Iwauchi, "Dielectric Properties of Fine Particles of Fe₃O₄ and Some Ferrites," *Japanese Journal Applied Physics*, Vol. 10, 1971, pp 1520-1528.
[doi:10.1143/JJAP.10.1520](https://doi.org/10.1143/JJAP.10.1520)
- [32] J. K. Park and D. Y. Kim, "Effect of Grain Size on Diffusion-Induced Grain-Boundary Migration in Ba(Zn_{1/3}-Nb_{2/3})O₃ Ceramics," *Journal American Ceramer Society*, Vol. 79, No. 5, 1996, pp. 1405-1415.
[doi:10.1111/j.1151-2916.1996.tb08604.x](https://doi.org/10.1111/j.1151-2916.1996.tb08604.x)
- [33] N. M. Burange, S. S. Chogule, D. R. Patil, R. S. Devan, Y. D. Koleka and B. K. Chougale, "Studies on Structural, Electrical and Magnetic Properties of γ (Ni_{0.5}Zn_{0.3}Co_{0.2}Fe₂O₄)+(1- γ)(BaTiO₃) Composites," *Journal of Alloys and Compounds*, Vol. 479, No. 1-2, 2009, pp. 569-573.
[doi:10.1016/j.jallcom.2009.01.004](https://doi.org/10.1016/j.jallcom.2009.01.004)